SUPPLEMENTAL EXPERIMENTAL PROCEDURES

Mice

Ksp-Cre transgenic mice (Shao et al., 2002) (*B6.Cg-Tg(Cdh16-cre)91Igr/J)* and *Vhl*$^{F/F}$ mice (Haase et al., 2001) (C;129S-*Vhl*^{tm1Jae}/J) were obtained from The Jackson Laboratory. *Pbrm1* $^{F/F}$ (*Baf180*$^{F/F}$) mice were obtained from Dr. Wang Zhong (Wurster et al., 2012). Three mouse strains were bred to generate *Vhl*$^{F/F}$*Ksp-Cre*, *Pbrm1*$^{F/F}$*Ksp-Cre*, and *Vhl*$^{F/F}$*Pbrm1*$^{F/F}$*Ksp-Cre.* All of the mice were on a mixed genetic background (B6, BALB/c, and 129). Animal experiments were performed in accordance to the Institutional Animal Care and Use Committee (IACUC) at the Memorial Sloan Kettering Cancer Center.

Mouse MRI

Mice MRI scans were carried out on either 200 or 300 MHz Bruker 4.7T or 7T Biospec scanners (Bruker Biospin MRI GmbH, Ettlingen, Germany) equipped with 640 mT/m ID 115 mm and 300 mT/m ID 200 mm gradients respectively (Resonance Research, Inc., Billerica, MA). RF excitation and acquisition were achieved by a custom-built quadrature birdcage resonator with ID of 32 mm (Stark Contrast MRI Coils Research Inc., Erlangen, Germany). The mice were immobilized with 1% isoflurane (Baxter Healthcare Corp., Deerfield, IL) gas in oxygen. Animal respiration was monitored with a small animal physiological monitoring system (SA Instruments, Inc., Stony Brook, New York). Scout images along three orthogonal orientations were first acquired for animal positioning. For mouse kidney imaging, coronal T2-weighted images using fast spin-echo RARE sequence (Rapid Acquisition with Relaxation Enhancement) were acquired with TR 1.5, TE 48 ms, RARE factor of 8, slice thickness of 0.7 mm, FOV 30 mm, in-plane resolution of 117 x 156 um, and 18 averages.

BUN and Creatinine Test

Blood was collected from mice using retro-orbital blood collection method. Serum was analyzed for BUN and creatinine concentration by the Laboratory of Comparative Pathology (LCP) on a Beckman Coulter AU680 analyzer.

Renal Subcapsular Allograft Tumor Implantation

Renal subcapsular allograft tumor implantation was performed as described previously (Sivanand et al., 2012). Briefly, the kidney tumors were harvested from the donor mice (*Vhl*$^{F/F}$*Pbrm1*$^{F/F}$*Ksp-Cre*) that were anesthetized by isoflurane. The tumors were transferred to a sterile dish with phosphate-buffered saline and cut into 8 to 27 mm^3 fragments. 6-8 weeks male *NOD*/*SCID*/IL2Rγ^{null} (NSG) mice were anesthetized and sterilized by Betadine and alcohol pads in preparation for implantation. The mice were then injected subcutaneously with 2 mg/kg of meloxicam and 0.5mg/kg buprenorphine to prepare for the surgery. A 8mm transverse incision was made to expose the kidneys, followed by a small incision (2mm) on the renal capsule. A pocket was carefully created underneath the renal capsule and the tumor fragments from the donor *Vhl*$^{F/F}$*Pbrm1*$^{F/F}$*Ksp-Cre* mice were then inserted carefully, after which wounds were closed and mice were closely monitored for healing and tumor development in accordance to the IACUC protocol.

Histopathology

Mouse kidneys were removed and fixed in 10% (vol/vol) neutral-buffered formalin overnight. The fixed kidneys were then processed in ethanol and xylene, embedded in paraffin, sectioned at 5 μm, and stained with hematoxylin and eosin (H&E). Selected slides were examined by board certified pathologists.

Immunohistochemistry

Paraffin-embedded tissues were sectioned at 5 μm and stained by the Pathology core at MSKCC. Immunohistochemistry (IHC) for pSTAT3, CA-IX, pS6K, THP, CD45, CD31, pERK, HIF1, HIF2, GLUT1, and p-4E-BP1 were conducted using Ventana Discovery XT (Ventana Medical Systems). Briefly, formalin-fixed, paraffin-embedded tissue was cut in 5 μm sections and air-dried overnight. The sections were deparaffinized, rehydrated, and subjected to heat-induced epitope retrieval (HIER). Sections were incubated with primary antibodies, including pSTAT3 (Cell Signaling Technology #9145/lot# ; dilution 1:50), CA-IX (Novo Biologic NB100-417/lot #O-1; dilution 1:8000), pS6K (Cell Signaling Technology #5364/lot 3122745), THP (Alfa Aesar BT 590/lot #590C14A; dilution 1:1000),

CD45 (BD 550539/lot #3122745), CD31 (Dako M0823/lot #12619/47), pERK (Cell Signaling Tecnology #4370/lot #7 dilution 1:1000), HIF1 (Cayman Chemical 10006421/lot #0484536-1; dilution 1:5000), HIF2 (gift from Dr. Ratcliffe; dilution 1:5000), GLUT1 (Cell Signaling Technology 12939S/lot #1; dilution 1:1000), and p4E-BP1 (Cell Signaling Technology #2855/lot #20; dilution 1:200). Slides were subjected to polymer treatment to avoid background staining of kidney tissue. For signal detection, the Omni anti Rb DAB HRP (Cat# 760-149) was used in accordance with manufacturers' instructions. Slides were counterstained with hematoxylin. Appropriate positive and negative controls were used for each run of IHC. IHC for Ki67 (Abcam ab16667;dilution 1:100, HIER at pH 9.0) and cleaved caspase-3 (Cell Signaling Technology #9661;1:250, HIER at pH 6.0) was performed by the Laboratory of Comparative Pathology (LCP) at MSKCC on a Leica Bond RX automated staining platform with a polymer detection system (Novocastra Bond Polymer Refine Detection, Leica Biosystems) and hematoxylin counter stain. TUNEL staining was performed by LCP at MSKCC (Gavrieli et al., 1992). Staining with fluorescein-conjugated lectins LTL (Vector Laboratories; dilution 1:100) was done on slides after rehydration and antigen retrieval for 4 hours at room temperature followed by DAPI counterstain and treatment with Sudan black.

RNA Isolation and Microarray Analysis

Total RNA was isolated using TRIzol (Life Technologies) and cleaned up using Qiagen column DNase digestion. RNA samples were prepared from three month old *Ksp-Cre*, *Vhl*$^{F/F}$*Ksp-Cre, Pbrm1*$^{F/F}$*Ksp-Cre*, and *Vhl*$^{F/F}$*Pbrm1*$^{F/F}$*Ksp-Cre* mice. Microarray was performed by Integrated Genomics Operation (IGO) at MSKCC. Briefly, double-stranded cDNA was synthesized from total RNA using the Affymetrix GeneChip cDNA synthesis kit according to the manufacturer's protocol. cDNA was then subjected to in vitro transcription, using the GeneChip IVT Labeling Kit. A measured aliquot of the biotinylated cRNA product was fragmented and hybridized along with the hybridization control kit onto the GeneChip (Mouse Gene 2.0 ST) genome array (Affymetrix). The hybridized biotinylated cRNA was stained with streptavidin-phycoerythrin (PE), and then

scanned with a GeneChip Array Scanner (Affymetrix). The fluorescence intensity of each probe was quantified using GeneChip Operating Software and GeneChip Analysis Suite (Affymetrix). Data were imported into R and preprocessed using the RMA algorithm. Differentially expressed genes were identified using limma and a Benjamini-Hochberg adjusted p-value cutoff (0.05) for the following conditions: *Vhl$^{F/F}$Ksp-Cre* vs *Ksp-Cre*, *Pbrm1$^{F/F}$Ksp-Cre* vs *Ksp-Cre*, *Vhl$^{F/F}$Pbrm1$^{F/F}$Ksp-Cre* vs *Ksp-Cre*, *Vhl$^{F/F}$Pbrm1$^{F/F}$Ksp-Cre* vs *Vhl$^{F/F}$Ksp-Cre*, or *Vhl$^{F/F}$Pbrm1$^{F/F}$Ksp-Cre* vs *Pbrm1$^{F/F}$Ksp-Cre*. Unsupervised hierarchical agglomerative clustering was then performed to identify clusters of differentially expressed genes. Four clusters that were identified using Pearson correlation and average linkage were further analyzed using ClueGO.

RNA Sequencing and Analysis

Total RNA was process by the IGO using TruSeq RNA Sample Prep kit according to the manufacturer's recommendation. Briefly, cDNA libraries were prepared from polyA selected RNA after end repair, A-tailing, ligation of the adaptors, and PCR enrichment. Libraries were later sequenced using Illumina HiSeq 2500 platform with 50 bp paired end reads and a total of 40 million reads per sample. The sequences obtained were mapped to the reference mouse genome using STAR (v2.3). Reads were then quantified using HTSeq-count and analyzed for differential expression using EdgeR. Genes that showed a corrected FDR < 0.05 were used for clustering and pathway analysis. Hierarchical agglomerative clustering was performed and displayed using heatmap.2() function in gplots package of R. A venn diagram was generated using Biovenn to visualize and compare the differentially expressed genes of mouse *Vhl$^{F/F}$Pbrm1$^{F/F}$Ksp-Cre* tumor versus normal (mP T/N), *Hif1α-M3* TRACK tumor versus normal (mH T/N), and TCGA-KIRC *VHL^{mt}PBRM1^{mt}* tumor versus normal (hT T/N) (Hulsen et al., 2008). Genes identified at the intersect of the venn diagram were further analyzed using ClueGO v2.1.6 (Bindea et al., 2009).

Gene ontology (GO) analysis of mouse microarray and RNA Sequencing data were performed with ClueGO using the following parameters:

Ontologies/Pathways-KEGG 07.05.2015; enrichment hypergeometric statistical test; correction method: Benjamini-Hochberg; GO term range levels: 3–8; minimal number of genes for term selection: 3; minimal percentage of genes for term selection: 4%; κ-score threshold: 0.4; group method: κ; minimal number of subgroups included in a group: 2; minimal percentage of shared genes between subgroups: 50%. The p value cut off of ClueGO for the clusters in microarrays was set to 0.0005. The ClueGO p value cut off for mP T/N, intersect of mP T/N and mH T/N, and intersect of all the three (mP, mH and hT T/N) were set to 0.005, 0.005, and 0.05 respectively. GSEA to discover gene sets enriched among DE genes in mP, mH, and mT T/N was performed using the JAVA GSEA 2.0 program (Subramanian et al., 2005). The gene sets used were Broad Molecular Signatures Database gene sets c2 (curated gene sets), as well as the additional curated genesets for HIF targets generated by merging the following published sets from msigdb- (Elvidge_Hypoxia_Up, Leonard_Hypoxia, Manalo_Hypoxia_Up, Maina_Hypoxia_VHL_Targets_Up, Pid_HIF1a_Pathway, Pid_HIF1_TFPathway, Semenza_HIF1_Targets, Lu_Tumor_Angiogenesis_Up). For testing the enrichment of the mTOR pathway, extended GSEA was performed to account for the direction of regulation of each gene in the gene set while calculating the enrichment. The extended GSEA was performed as described(Lim et al., 2009).

Reverse transcription and quantitative PCR

Total RNA was isolated from three month old *Ksp-Cre*, *Vhl$^{F/F}$Ksp-Cre,* *Pbrm1$^{F/F}$Ksp-Cre,* and *Vhl$^{F/F}$Pbrm1$^{F/F}$Ksp-Cre* mice as described above. Reverse transcription was performed with oligo-dT plus random decamer primers (Ambion) using Superscript II (Life Technologies). Quantitative PCR was performed with SYBR green master mix (Applied Biosystems) in duplicates using the indicated gene specific primers. Quantitative PCR was performed on a ViiA™ 7 Real-Time PCR System (Applied Biosystems). Gene specific primers are listed in Supplementary Table 8. Data were analyzed as described previously by normalization against GAPDH or 18S rRNA.

Motif Activity Analysis

To analyze activities of transcription factor binding motifs (TFBM) using RNA-seq data, we used the Integrated System for Motif Activity Response Analysis (ISMARA) (Balwierz et al., 2014). This method uses motif activity response analysis to determine the transcription factors that drive the observed changes in target gene expression across samples

HOMER was used to find transcription factor motifs in the different clusters that were identified using unsupervised hierarchical clustering of microarray data that was performed on the three month old *Ksp-Cre*, *Vhl$^{F/F}$Ksp-Cre, Pbrm1$^{F/F}$Ksp-Cre, Vhl$^{F/F}$Pbrm1$^{F/F}$Ksp-Cre* mice. We searched for significantly enriched 8-10 nt sequence motifs with the Hypergeometric Optimization of Motif EnRichment program (HOMER) compared to the background genome sequence in the promoter regions (-1kb upstream from TSS, 100bp downstream from TSS).

REFERENCES

Balwierz, P. J., Pachkov, M., Arnold, P., Gruber, A. J., Zavolan, M., and van Nimwegen, E. (2014). ISMARA: automated modeling of genomic signals as a democracy of regulatory motifs. Genome Res *24*, 869-884.

Bindea, G., Mlecnik, B., Hackl, H., Charoentong, P., Tosolini, M., Kirilovsky, A., Fridman, W. H., Pages, F., Trajanoski, Z., and Galon, J. (2009). ClueGO: a Cytoscape plug-in to decipher functionally grouped gene ontology and pathway annotation networks. Bioinformatics *25*, 1091-1093.

Gavrieli, Y., Sherman, Y., and Ben-Sasson, S. A. (1992). Identification of programmed cell death in situ via specific labeling of nuclear DNA fragmentation. J Cell Biol *119*, 493-501.

Haase, V. H., Glickman, J. N., Socolovsky, M., and Jaenisch, R. (2001). Vascular tumors in livers with targeted inactivation of the von Hippel-Lindau tumor suppressor. Proc Natl Acad Sci U S A *98*, 1583-1588.

Hulsen, T., de Vlieg, J., and Alkema, W. (2008). BioVenn - a web application for the comparison and visualization of biological lists using area-proportional Venn diagrams. BMC Genomics *9*, 488.

Lim, W. K., Lyashenko, E., and Califano, A. (2009). Master regulators used as breast cancer metastasis classifier. Pac Symp Biocomput, 504-515.

Shao, X., Somlo, S., and Igarashi, P. (2002). Epithelial-specific Cre/lox recombination in the developing kidney and genitourinary tract. J Am Soc Nephrol *13*, 1837-1846.

Sivanand, S., Pena-Llopis, S., Zhao, H., Kucejova, B., Spence, P., Pavia-Jimenez, A., Yamasaki, T., McBride, D. J., Gillen, J., Wolff, N. C.*, et al.* (2012). A validated tumorgraft model reveals activity of dovitinib against renal cell carcinoma. Sci Transl Med *4*, 137ra175.

Subramanian, A., Tamayo, P., Mootha, V. K., Mukherjee, S., Ebert, B. L., Gillette, M. A., Paulovich, A., Pomeroy, S. L., Golub, T. R., Lander, E. S., and Mesirov, J. P. (2005). Gene set enrichment analysis: a knowledge-based approach for interpreting genome-wide expression profiles. Proc Natl Acad Sci U S A *102*, 15545-15550.

Wurster, A. L., Precht, P., Becker, K. G., Wood, W. H., 3rd, Zhang, Y., Wang, Z., and Pazin, M. J. (2012). IL-10 transcription is negatively regulated by BAF180, a component of the SWI/SNF chromatin remodeling enzyme. BMC Immunol *13*, 9.

Supplementary Figures

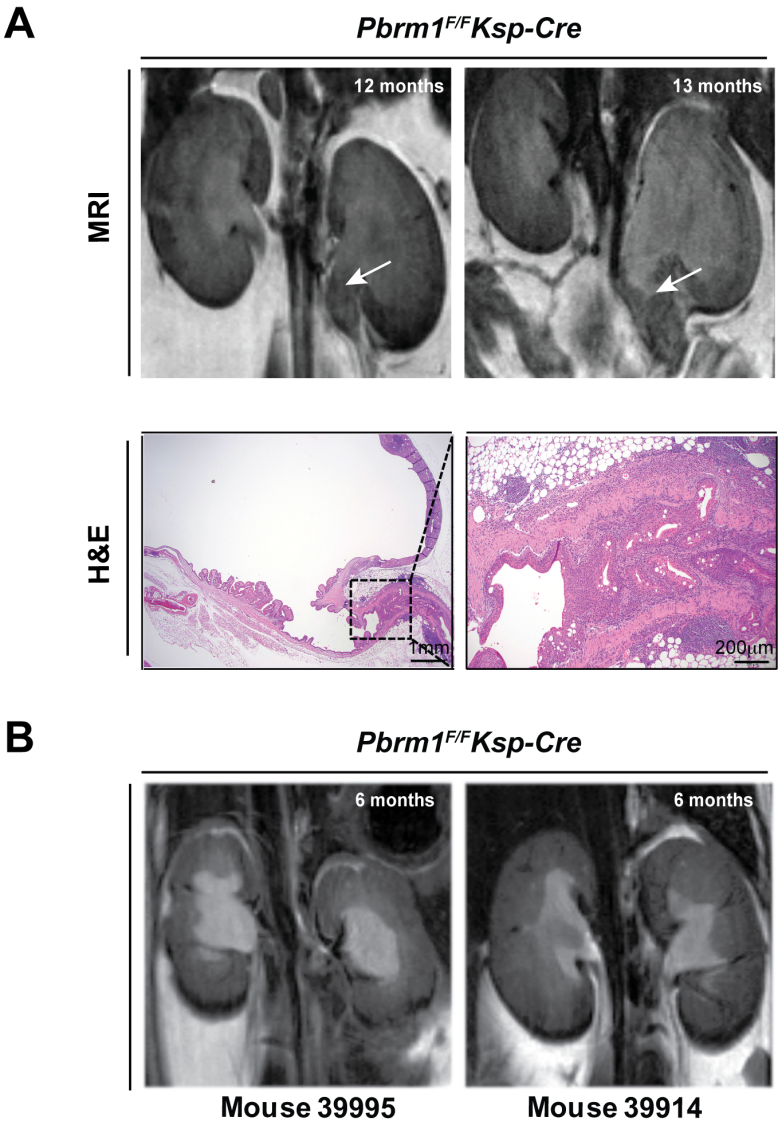

Supplementary Figure S1. ***Pbrm1$^{F/F}$Ksp-Cre*** **Mice Develop Obstructive Hydronephrosis,** Related to Figure1. (A) MRI images of a *Pbrm1$^{F/F}$Ksp-Cre* mouse with severe hydronephrosis at 12 months and 13 months of age. White arrows denote the non-neoplastic mass at the proximal ureter. Hematoxylin & eosin (H&E)-stained sections of the *Pbrm1$^{F/F}$Ksp-Cre* hydronephrotic kidney at the ureteroplevic junction. Insert is the blowup image of the benign obstructive

mass occluding the proximal ureter. (B) MRI images of early hydronephrosis in two *Pbrm1* $^{F/F}$*Ksp-Cre* mice at 6 months of age.

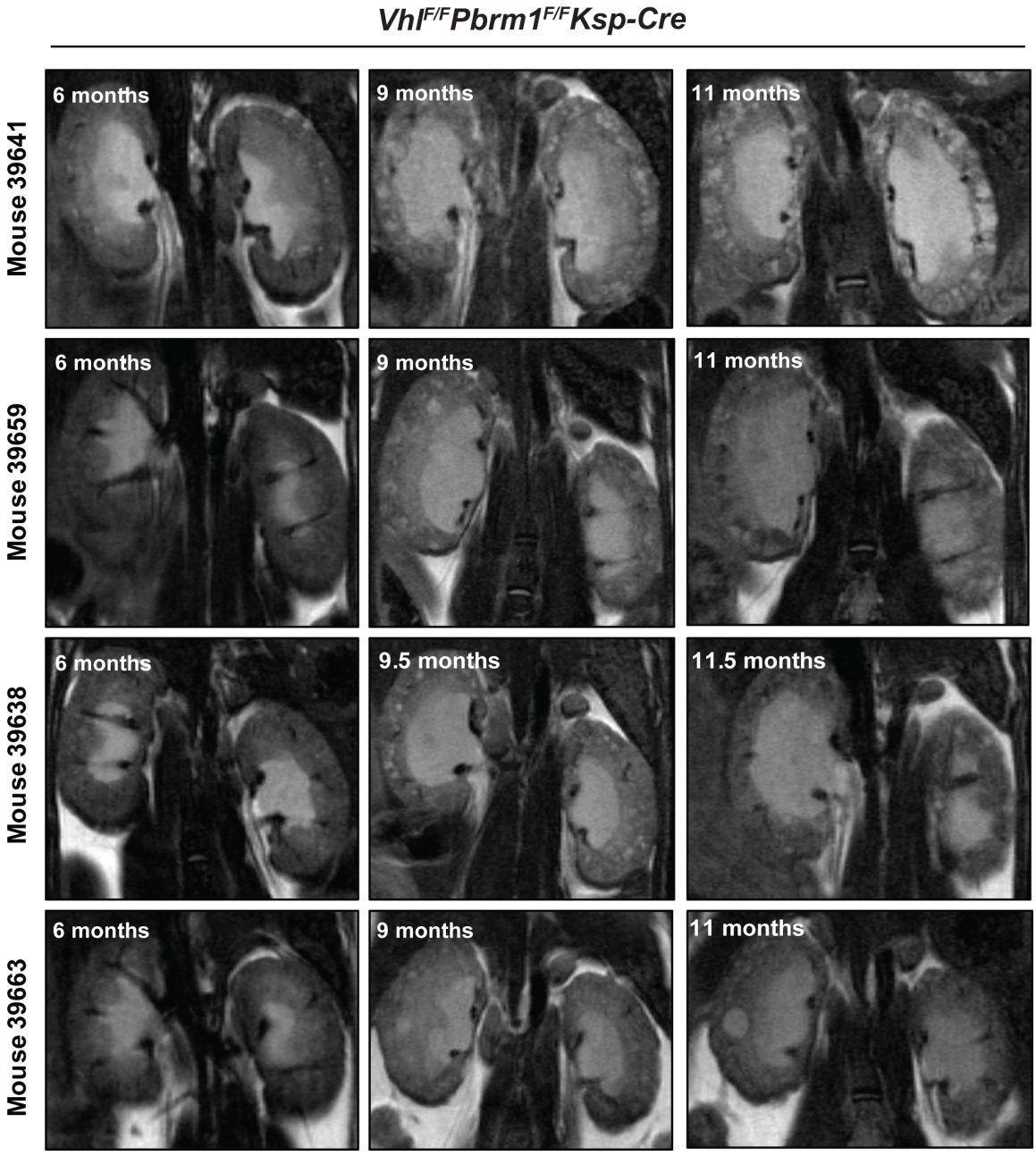

Supplementary Figure S2. ***Vhl*** $^{F/F}$***Pbrm1*** $^{F/F}$***Ksp-Cre*** **Mice Develop Polycystic Kidney Disease** Related to Figure2. MRI images of four *Vhl* $^{F/F}$*Pbrm1* $^{F/F}$*Ksp-Cre* mice at the indicated age.

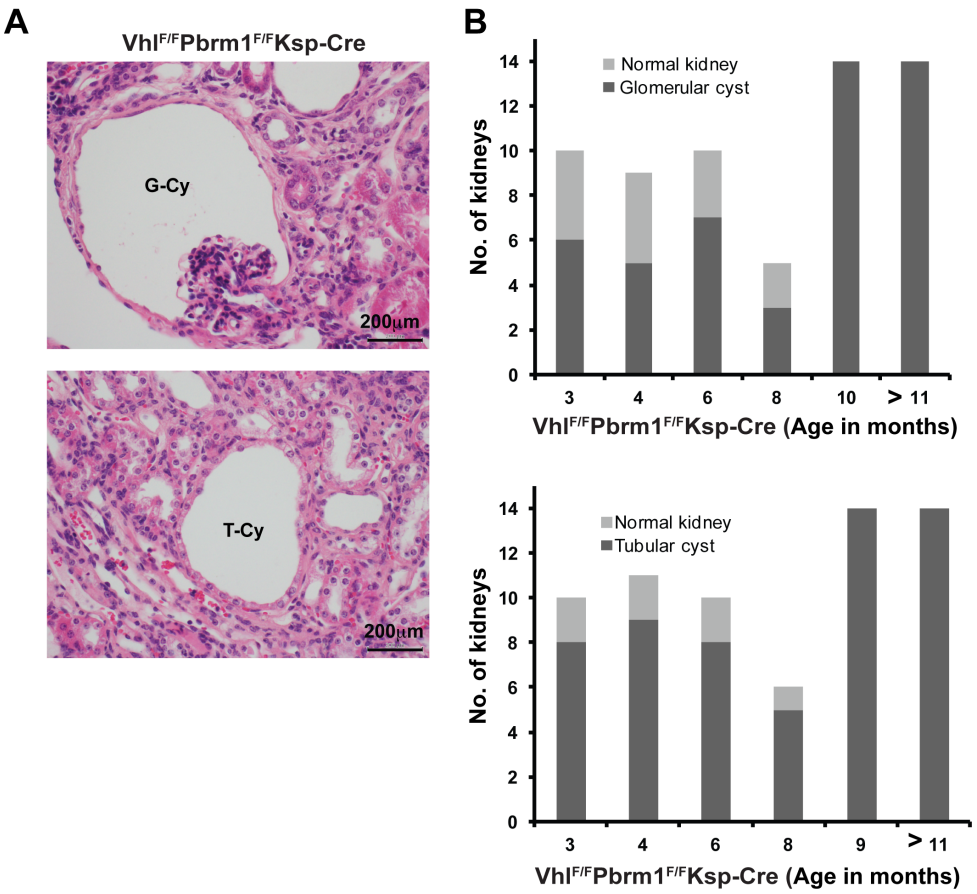

Supplementary Figure S3. ***Vhl$^{F/F}$Pbrm1$^{F/F}$Ksp-Cre*** **Mice show Glomerular and Tubular Cysts,** Related to Figure2. (A) H&E staining of kidney sections from *Vhl$^{F/F}$Pbrm1$^{F/F}$Ksp-Cre* mice. Bright-field photographs of tubular (top panel) and glomerular (bottom panel) cyst from *Vhl$^{F/F}$Pbrm1$^{F/F}$Ksp-Cre* kidneys at 200μm. G-Cy, glomerular cysts; T-Cy, tubular cyst. (B) Incidence of the microscopic cysts detected in kidney cortex of *Vhl$^{F/F}$Pbrm1$^{F/F}$Ksp-Cre*. Columns, number of mice with normal (light grey) or cystic (dark grey) kidney cortex.

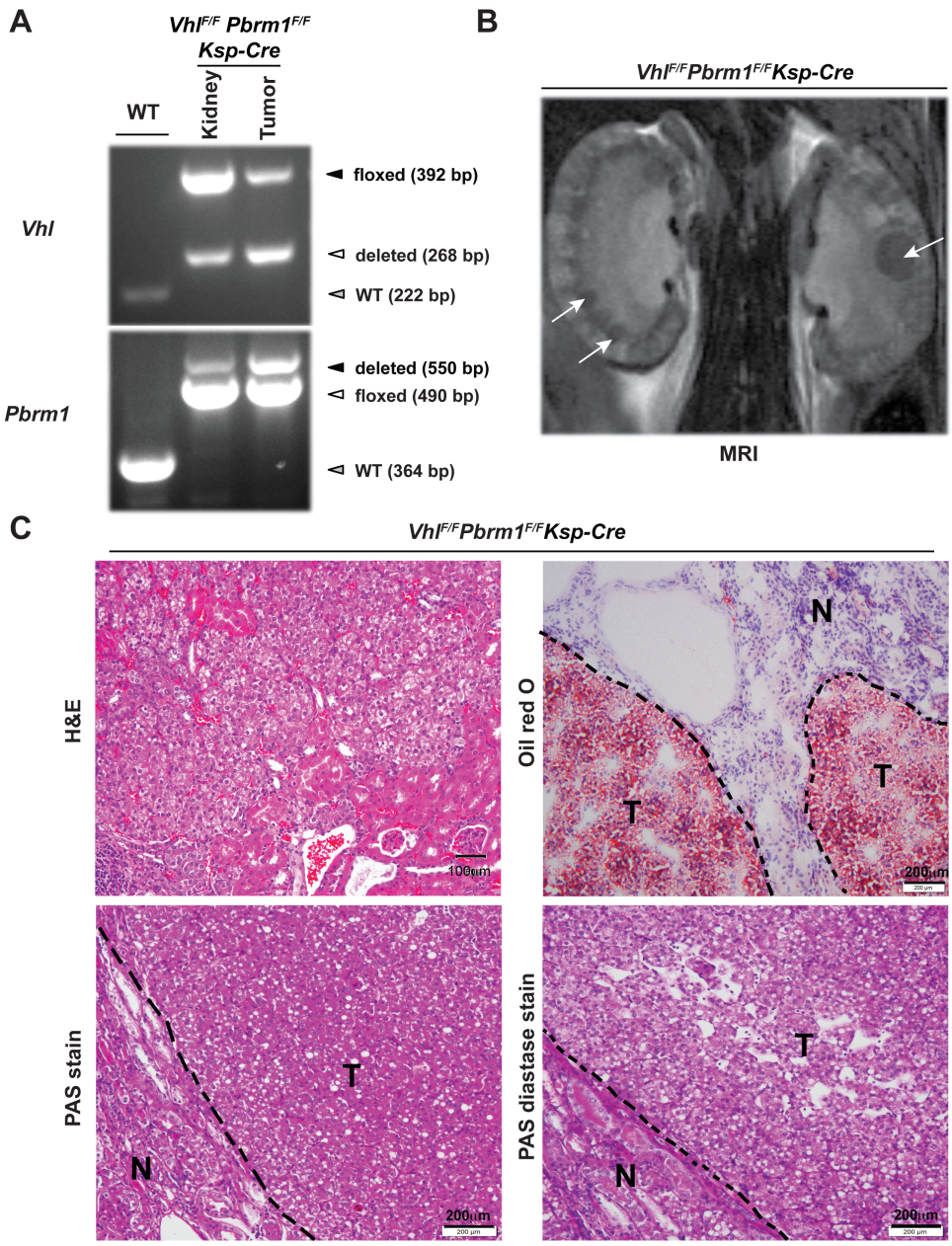

Supplementary Figure S4. ***Vhl*$^{F/F}$*Pbrm1*$^{F/F}$*Ksp-Cre* Mice Develop Multifocal Clear Cell Kidney Cancers,** Related to Figure3. (A) PCR genotyping of DNA obtained from WT kidney, *Vhl*$^{F/F}$*Pbrm1*$^{F/F}$*Ksp-Cre* kidney, or *Vhl*$^{F/F}$*Pbrm1*$^{F/F}$*Ksp-Cre* kidney tumor. (B) A representative MRI image of *Vhl*$^{F/F}$*Pbrm1*$^{F/F}$*Ksp-Cre* kidneys with multifocal tumors indicated by arrows. (C) A representative H&E (top left panel), Oil red O (top right panel), PAS (bottom left panel), and PAS Diastase (bottom right) -stained sections of *Vhl*$^{F/F}$*Pbrm1*$^{F/F}$*Ksp-Cre* kidney tumor demonstrated classical ccRCC histological features.

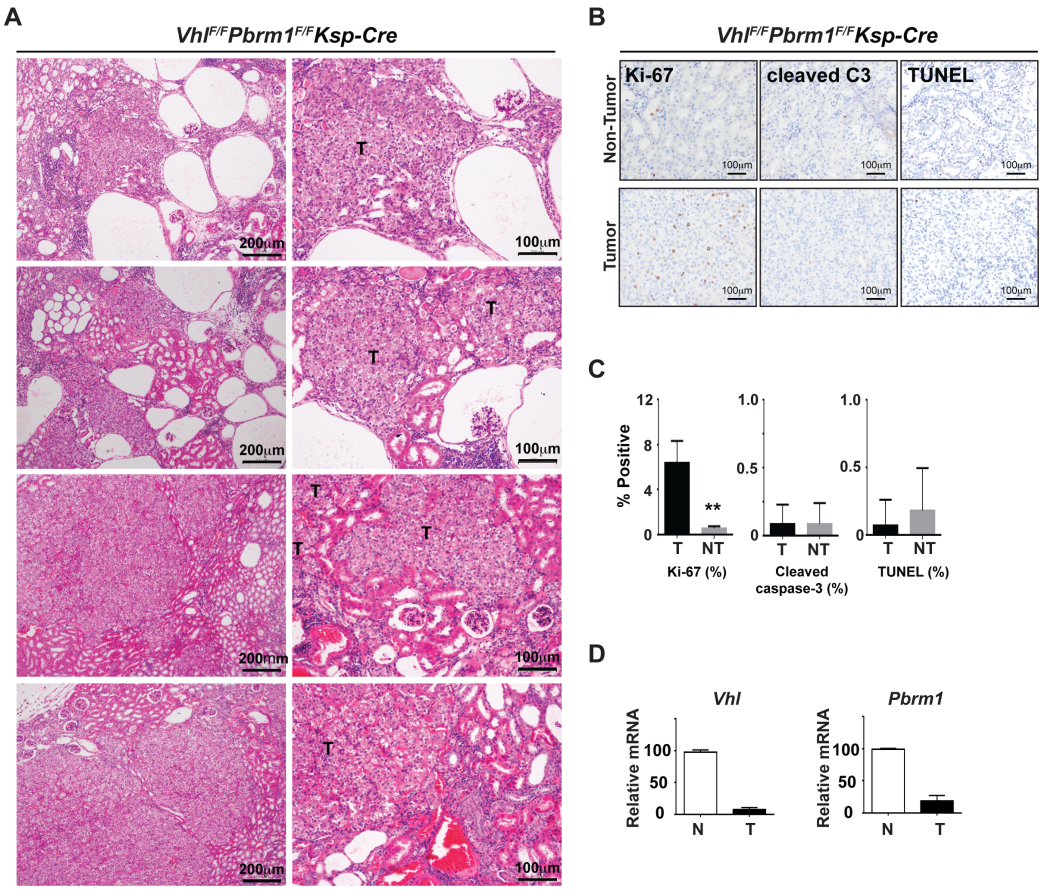

Supplementary Figure S5. ***Vhl*$^{F/F}$*Pbrm1*$^{F/F}$*Ksp-Cre* Mice Tumors do not Originate from Cystic Lesion,** Related to Figure3. (A) Representative hematoxylin & eosin (H&E)-stained sections of *Vhl*$^{F/F}$*Pbrm1*$^{F/F}$*Ksp-Cre* kidney tumors. (B) Representative images of immunohistochemistry of Ki-67, immunohistochemistry of cleaved caspase-3 (cleaved C3), and TUNEL staining in the tumor areas and adjacent non-tumor tissues of *Vhl*$^{F/F}$*Pbrm1*$^{F/F}$*Ksp-Cre* mouse. (C) Quantification of the Ki-67, cleaved Caspase-3, and TUNEL staining in (B). Three microscopic fields were randomly selected and the percentage of positively stained cells divided by the total number of cells counted was calculated. Data shown is the average derived from kidney sections of 3 or more different mice. **, $P < 0.01$. (D) The mRNA levels of *Vhl* and *Pbrm1* in the *Vhl*$^{F/F}$*Pbrm1*$^{F/F}$*Ksp-Cre* tumors or aged-matched WT mice were assessed by qRT-PCR. Data were normalized against 18S rRNA (mean ± s.d., n=3 independent experiments). ***, $P < 0.0001$ (Student's *t*-test).

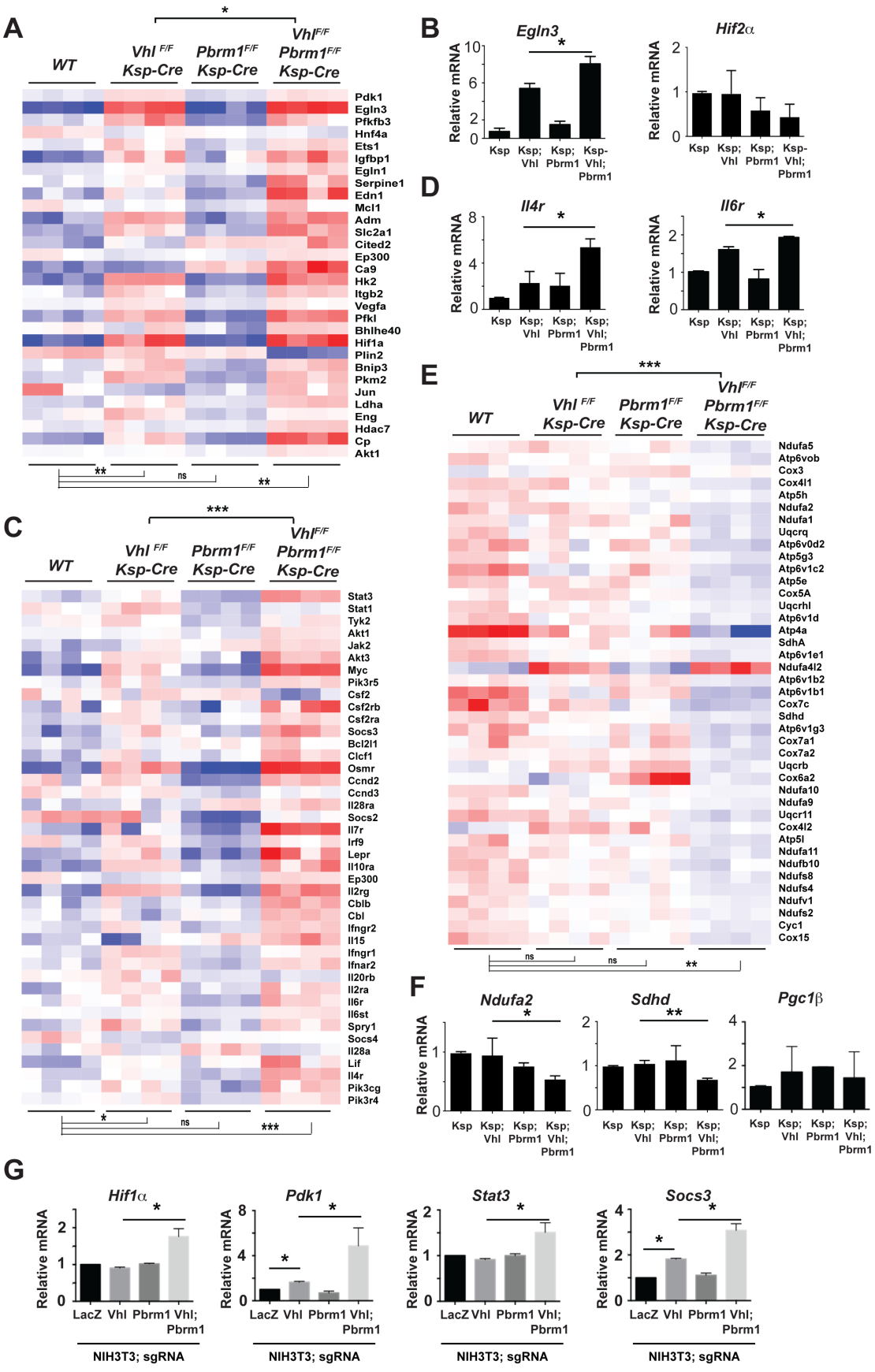
A
WT
Vhl F/F Ksp-Cre
Pbrm1F/F Ksp-Cre
VhlF/F Pbrm1F/F Ksp-Cre
Pdk1
Egln3
Pfkfb3
Hnf4a
Ets1
Igfbp1
Egln1
Serpine1
Edn1
Mcl1
Adm
Slc2a1
Cited2
Ep300
Ca9
Hk2
Itgb2
Vegfa
Pfkl
Bhlhe40
Hif1a
Plin2
Bnip3
Pkm2
Jun
Ldha
Eng
Hdac7
Cp
Akt1
B
Egln3
Hif2α
Relative mRNA
Ksp
Ksp; Vhl
Ksp; Pbrm1
Ksp-Vhl; Pbrm1
C
Stat3
Stat1
Tyk2
Akt1
Jak2
Akt3
Myc
Pik3r5
Csf2
Csf2rb
Csf2ra
Socs3
Bcl2l1
Clcf1
Osmr
Ccnd2
Ccnd3
Il28ra
Socs2
Il7r
Irf9
Lepr
Il10ra
Ep300
Il2rg
Cblb
Cbl
Ifngr2
Il15
Ifngr1
Ifnar2
Il20rb
Il2ra
Il6r
Il6st
Spry1
Socs4
Il28a
Lif
Il4r
Pik3cg
Pik3r4
D
Il4r
Il6r
E
Ndufa5
Atp6vob
Cox3
Cox4l1
Atp5h
Ndufa2
Ndufa1
Uqcrq
Atp6v0d2
Atp5g3
Atp6v1c2
Atp5e
Cox5A
Uqcrhl
Atp6v1d
Atp4a
SdhA
Atp6v1e1
Ndufa4l2
Atp6v1b2
Atp6v1b1
Cox7c
Sdhd
Atp6v1g3
Cox7a1
Cox7a2
Uqcrb
Cox6a2
Ndufa10
Ndufa9
Uqcr11
Cox4l2
Atp5l
Ndufa11
Ndufb10
Ndufs8
Ndufs4
Ndufv1
Ndufs2
Cyc1
Cox15
F
Ndufa2
Sdhd
Pgc1β
G
Hif1α
Pdk1
Stat3
Socs3
LacZ
Vhl
Pbrm1
Vhl; Pbrm1
NIH3T3; sgRNA

Supplementary Figure S6. **Amplification of the Transcriptional Outputs of HIF1 and STAT3 Incurred by VHL Loss after PBRM1 Loss,** Related to Figure5; Table S2a,2b. (A) Heat map of the genes from the PID HIF1 pathway (MSigDB) are plotted for the indicated genotypes. Enhancement of HIF1 signature in *Vhl*$^{F/F}$*Pbrm1*$^{F/F}$*Ksp-Cre* was tested using Fisher's exact test. *, $P < 0.05$ (B) The mRNA levels of the indicated genes from the indicated genotypes were assessed by qRT-PCR. Data were normalized against GAPDH (mean± s.d., n=3 independent experiments). *, $P < 0.05$; **, $P < 0.005$ (Student *t*-test). (C) Heat map of the genes from the KEGG JAK-STAT Signaling pathway (MSigDB) are plotted for the indicated genotypes. Enhancement of STAT3 signature in *Vhl*$^{F/F}$*Pbrm1*$^{F/F}$*Ksp-Cre* was tested using Fisher's exact test. ***, $P < 0.0005$. (D) The mRNA levels of the indicated genes from the indicated genotypes were assessed by qRT-PCR. Data were normalized against GAPDH (mean± s.d., n=3 independent experiments). *, $P < 0.05$ (Student *t*-test). (E) Heatmap of the genes from the KEGG Oxidative Phosphorylation pathway (MSigDB) are plotted for the indicated genotypes. Downregulation of these genes in *Vhl*$^{F/F}$*Pbrm1*$^{F/F}$*Ksp-Cre* was tested using Fisher's exact test. ***, $P < 0.0005$ (F) The mRNA levels of the indicated genes from the indicated genotypes were assessed by qRT-PCR. Data were normalized against GAPDH (mean± s.d., n=3 independent experiments). **, $P < 0.005$ (Student *t*-test). (G) The mRNA levels of the indicated genes from NIH3T3 cells that were knock out for indicated genes by qRT-PCR. Data were normalized against GAPDH (mean± s.d., n=3 independent experiments). **, $P < 0.005$ (Student *t*-test).

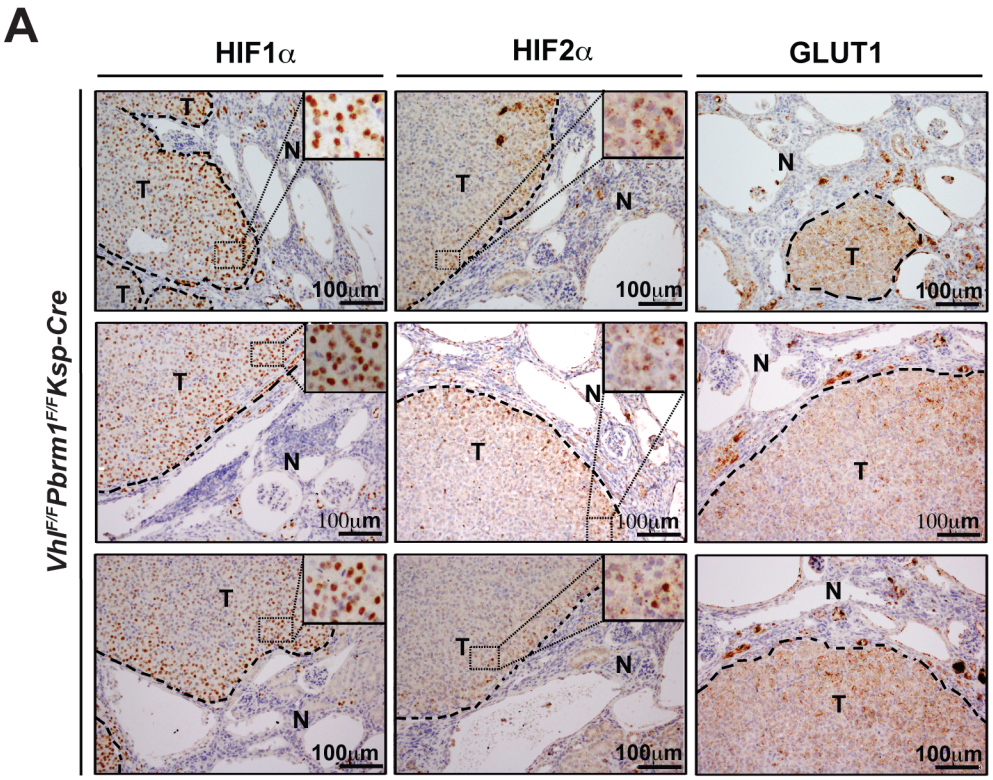

Supplementary Figure S7. *Vhl* and *Pbrm1* Doubly Deficient Clear Cell Kidney Tumors Display significantly high HIF and mTORC1 Signaling, Related to Figure6. (A) Representative immunohistochemistry images of HIF1α (column 1), HIF2α (column 2), and GLUT1 in *Vhl$^{F/F}$Pbrm1$^{F/F}$Ksp-Cre* tumors. T and N denote Tumor and adjacent Normal, respectively. Scale bars are at 100μm as indicated. (B) Immunoblots of protein lysates prepared from wild-type and *Vhl$^{F/F}$Pbrm1$^{F/F}$Ksp-Cre* kidney tumors probed for p-4EBP1 (top panel) and total 4EBP1 (middle panel). Actin (bottom panel) serves as a loading control.

Supplementary Tables

Table S1. Gross and histopathological analyses of mice, Related to Figure 3, Figure S4, Figure S5.

Table S2a. Genes that are differentially expressed in 12 week-old mice across the indicated genotypes (WT, $Vhl^{F/F}$Ksp-Cre, $Pbrm1^{F/F}$Ksp-Cre, and $Vhl^{F/F}Pbrm1^{F/F}$Ksp-Cre) as determined by Microarray, Related to Figure 5, Figure S6.

Table S2b. KEGG pathways overrepresented in the clusters identified by unsupervised hierarchical clustering of differentially expressed genes in 12 week-old mice across the genotypes (*WT*, *$Vhl^{F/F}$Ksp-Cre*, *$Pbrm1^{F/F}$Ksp-Cre,* and *$Vhl^{F/F}Pbrm1^{F/F}$Ksp-Cre*) tested by ClueGO, Related to Figure 5, Figure S6.

Table S3: Genes that are differentially expressed among five $Vhl^{F/F}Pbrm1^{F/F}$Ksp-Cre tumor samples and four age-matched WT normal kidney samples determined by RNASeq, Related to Figure 6.

Table S4. KEGG pathways overrepresented in the genes that are differentially expressed among five $Vhl^{F/F}Pbrm1^{F/F}$Ksp-Cre tumor samples and four age-matched WT normal kidney samples as tested by ClueGO, Related to Figure 6.

Table S5. KEGG pathways overrepresented in the set of differentially expressed genes that is common between $Vhl^{F/F}Pbrm1^{F/F}$Ksp-Cre mouse ccRCC tumors versus normal and Hif1α-M3 TRACK mouse ccRCC tumors versus normal as determine by ClueGO, Related to Figure 7.

Table S6. KEGG pathways overrepresented in the shared differentially expressed genes between $Vhl^{F/F}Pbrm1^{F/F}$Ksp-Cre mouse ccRCC tumors versus

normal, Hif1α-M3 TRACK mouse ccRCC tumors versus normal, and TCGA $VHL^{mt}PBRM1^{mt}$ human ccRCC tumor versus normal as determine by ClueGO. Related to Figure 7.

Table S7. Primers for qRT-PCR, Related to Figures 5-6, Figures S5-6.